Identifying a gene orchestrating skin regeneration via tissue rebuilding
~ Inspiration from aesthetic treatments ~

Satomi, Kiuchi[1]; Takaya, Oishi[1]; Yuki, Cho[1]; Tiago J.S. Lopes[2]; Hiroko, Ochiai[3]; **Takamasa, Gomi**[1*];

[1] POLA Chemical Industries, Inc., Yokohama, Japan; [2] Center of Regenerative Medicine, National Center for Child Health and Development Research Institute, Tokyo, Japan;
[3] National Hospital Organization Tokyo Medical Center, Tokyo, Japan

* Takamasa Gomi, 560 Kashio-cho Totsuka-ku Yokohama Japan, +81-45-826-7231, takag@pola.co.jp

Abstract

Background: Aesthetic treatments lead to certain skin improvement, but they are often damaging to the skin. Following damage, the treated skin is remodeled, and the fibrous structures show histological rejuvenation (different from wounding damage, that often results in the formation of fibrotic scar tissue). Although both phenomena are caused by tissue damage, the underlying mechanism of this histological rejuvenation is unclear. Here, we studied the biological responses that occur after aesthetic treatment and identified a key gene that triggers tissue remodeling.

Methods: We established a comprehensive analysis system where fresh human subcutaneous adipose tissue was co-cultured with adipose-derived stem cells (ASCs). We observed changes in fibrous structures that occurred over time using microscopy, and used a combination of gene expression and computational analyses to identify the key regulatory genes involved in tissue remodeling.

Results: Microscopic observation revealed that the presence of ASCs induced transient degradation and subsequent synthesis of type I collagen in subcutaneous adipose tissue. We identified TSG-6 as a central component in the human protein-protein interaction network, and this paracrine factor eased the inflammatory state of tissues and promoted collagen replacement *ex vivo*. Importantly, TSG-6 inhibited the formation of neutrophil extracellular traps (NETs), which act in a pro-fibrotic manner against subcutaneous adipose tissue.

Conclusion: Together, our findings point towards the exciting possibility of designing cosmetics with superior efficacy for restoring the skin's fibrous structures. Overall, the discovery of novel molecular targets that induce rejuvenation will revolutionize the cosmetics field.

Keywords: Tissue remodeling; Biological network analysis; Adipose-derived stem cells; Neutrophil extracellular traps; RNA sequencing

1. Introduction

Fibrous structures are dominant components of the skin, which influences its appearance. Skin fibrous structures are composed of extracellular matrix (ECM) components such as collagen, elastin, and proteoglycans, which provide mechanical strength, elasticity, and moisture to the skin [1]. However, these functions are going down in aged or photoaged skin due to changes in fibrous structures (e.g., reduction of amount of fibers present or the accumulation of degraded old fibers without replacement by new ones) [2], [3]. As these phenomena reduce the skin's ability to support itself, problems such as wrinkling and sagging begin to appear. Therefore, it is important to maintain the function of the fibrous structures.

Old fibrous structures which have accumulated have been considered difficult to remove, with the exception of certain aesthetic treatments by physicians. The injection of adipose-derived stem cells (ASCs) subcutaneously is the aesthetic treatment that can make this possible [4]. Previous reports have shown that this treatment remarkably improves aging-related skin problems [5], and the mechanism is considered not only physical replenishment but also biological responses that remove abnormal fibrous structures and replace them with new ones. This is based on the finding that in treated skin, dermal elastosis is reduced, elastic fibers are regenerated, and fibrous structures around fat are normalized, resulting in a histologically rejuvenated phenotype [6]. Moreover, the ASCs injection treatment also improves skin fibrosis caused by X-irradiation [7]. However, studies explaining the underlying mechanisms of the biological responses in the ASCs-injected skin are still scarce. The aesthetic treatment involves damage to the skin, but wounding damage to the skin often results in fibrotic scar formation. It is unclear how the aesthetic treatment achieves tissue remodeling.

In this study, we identified a key gene that directs tissue remodeling by elucidating a series of biological responses that occur in ASCs-injected skin using an *ex vivo* experimental model. Our results suggest that by applying these findings, cosmetics will have novel functions to induce tissue remodeling. We call this concept *Rebuilding Induction,* and expect expanding what can be achieved with cosmetics.

2. Materials and Methods

2.1. Human subcutaneous adipose tissue samples

Abdominal subcutaneous adipose tissue from Japanese volunteers were obtained at the National Hospital Organization Tokyo Medical Center. The study was approved by the ethical committees of the National Hospital Organization Tokyo Medical Center (R17-209) and POLA Chemical Industries, Inc. (2018-G-032), conducted in accordance with the Declaration of Helsinki. All subjects provided written consent. The collected samples were transferred to the analysis institution in a collection tube with sterile phosphate buffered saline (PBS) (FUJIFILM Wako Pure Chemical, Tokyo, Japan) under temperature-retaining conditions. The samples were cut into 3-6 mm pieces, disinfected, and washed in sterile PBS, and culture began within several hours of harvest.

Cheek subcutaneous adipose tissue from Caucasian females was purchased from Obio, LLC. (El Segundo, CA).

2.2. Cell culture

Human ASCs (PT-5006, Lonza, Basel, Switzerland) were cultured in Adipose-Derived Stem Cells Basal Medium (Lonza) at 37℃ with 5% CO2. When cells reached 80% confluence, cells were subcultured in 6-well culture plates at a density of 4.5×10^4 cells per well.

Human neutrophils (PB011C-1, HemaCare, Northridge, CA) were cultured in RPMI 1640 Medium (Thermo Fisher Scientific, Waltham, MA) containing 10% fetal bovine serum (FBS) (MoregateBiotech, Bulimba, Queensland) and 2 mM L-Glutamine (Thermo Fisher Scientific) at 37℃ with 5% CO2.

2.3. ASCs co-cultured *ex vivo* experimental model

Fresh subcutaneous adipose tissue was cultured in 6-well culture plate seeded with ASCs. The media was changed to Dulbecco's Modified Eagle Medium/Ham Nutrient Mixture F-12 (DMEM/F-12) (Merck, Darmstadt, Germany) containing 10% FBS and 2.5× Antibiotic-Antimycotic Mixed Solution (Nacalai Tesque, Kyoto, Japan). As a control group, the tissue cultured without ASCs were used. Plates were cultured for up to 7 days at 37℃ with 5% CO2. The culture medium was changed every 3 days.

To inhibit TSG-6 function, 2.5 ng/mL goat anti-TSG-6 antibody (R&D systems, Minneapolis, MN) was added to the medium. Normal Goat IgG (R&D systems) was used as a control.

2.4. Gene expression analysis

Total RNA was extracted from subcutaneous adipose tissues with the RNeasy Lipid Tissue Mini Kit (Qiagen, Hilden, Germany) according to the manufacturer's instructions.

RNA sequencing libraries were generated and sequenced by Azenta Life Sciences (Chelmsford, MA) using NovaSeq 6000 (Illumina, San Diego, CA). Raw data were converted to Fastq format. Quality control was performed using FastQC (version 0.10.1) [8]. Mapping the clean reads to the reference genome was performed using Hisat2 (version 2.0.1) [9]. Assessing the expression levels of mRNAs by calculating the fragments per kilobase of exon per million mapped reads (FPKM) was performed using HT-seq (version 0.6.1) [10]. Gene differential analysis was performed using the Bioconductor package DESeq2 (version 1.26.0) [11], and differentially expressed genes (DEGs) were determined according to the criteria of fold change greater than 1.5 and false discovery rate (FDR) less than 0.05. Gene Ontology (GO) enrichment of DEGs was analyzed using Enrichr (version 3.0) [12], [13]. The protein-protein interaction network of DEGs was predicted and constructed using Human Integrated Protein-Protein Interaction rEference (HIPPIE) (version 2.2) [14]. Then, Cytoscape software (version 3.8.2) [15] was utilized to visualize the network and calculate the score of degree centrality.

For quantitative polymerase chain reaction (qPCR), total RNA was reversed-transcribed into complementary DNA (cDNA) with Superscript VILO cDNA Synthesis kit (Thermo Fisher Scientific), and cDNA was amplified by QuantiTect SYBR Green PCR Kits (Qiagen). Pre-designed primers for detecting collagen type I alpha 1 (COL1A1), actin alpha 2, smooth muscle (ACTA2) and actin beta (ACTB) as an internal control were purchased from Qiagen.

2.5. Confocal fluorescence assay

Each subcutaneous adipose tissue sample was embedded in 2.5% agarose XP (NIPPON GENE, Tokyo, Japan) dissolved in sterile PBS. The embedded tissues were flattened by cutting in half using a razor and placed flattened side down in a 24 well culture insert (Merck).

A hole was punched in the center of the culture insert with a biopsy (ø3.0 mm, KAI, Tokyo, Japan) beforehand so that a portion of the flattened tissue was exposed.

To detect collagen degradation, the Cy3-conjugated collagen hybridizing peptide (CHP) (3Helix, Salt Lake City, UT) was used. After reconstituting CHP solution at the defined concentration with sterile PBS, heat the solution at 80°C for 5 min. The culture insert embedded tissue was immersed in staining solution containing 5 µM CHP and 1 µg/mL Hoechst 33342 (DOJINDO, Kumamoto, Japan), and incubated for 1 hour at 37℃ with 5% CO2.

To detect collagen synthesis, the embedded tissues were immunolabelled with rat anti-Procollagen Type I Antibody (1:500, Merck) for overnight followed by secondary antibody (Alexa Fluor Plus donkey anti-rat 488, 1:500, Thermo Fisher Scientific) and 1 µg/mL Hoechst 33342 for 2 hours at 37℃ with 5% CO2.

After each staining, the culture insert was transferred to a 6 well-glass bottom culture plate containing FluoroBrite DMEM (Thermo Fisher Scientific). The multi-stack images of the embedded tissues were obtained with the laser confocal microscope (A1R+, Nikon, Tokyo, Japan). Tissues were cultured after observation, and fluorescently stained and under observation again after several days of the culture. Collagen degradation was evaluated after 3 days and collagen synthesis was evaluated after 7 days of culture. In the second observations, a multi-stacked image of the same area was obtained. The imaging conditions on each channel were kept consistent.

The obtained 3D images were projected in 2D to create a maximum intensity projection (MIP) image. By Image J, the RGB images were converted to grayscale and a binarized, calculated the stained area value. The fibrous structural change was evaluated by the increasing ratio of area values. 3D images were created using Imaris (version 9.2.1, Carl Zeiss, Germany)

2.6. Neutrophil extracellular traps (NETs) induction, detection, and quantification

Neutrophils (1×10^6 cells/mL) were seeded in 13 mm poly-D-lysine charged glass coverslips within 24-well plate by centrifugation for 3 min at 300 ×g. The cells were pre-cultured with or without Recombinant Human TSG-6 Protein (31.25-250 pg/mL, R&D systems) for 15 min as necessary. Subsequently, the cells were incubated with phorbol-12-

myristate-13-acetate (PMA) (50 nM, FUJIFILM Wako Pure Chemical) for 1 hour to induce the formation of NETs.

The supernatant containing NETs was collected after centrifugation for 3 min at 300 ×g. When the collected supernatant was used for co-culture with tissue, before centrifugation, cells were gently washed and replaced with medium to prevent PMA carryover. Quant-iT PicoGreen dsDNA Assay Kit (Thermo Fisher Scientific) was used to measure the DNA concentration in the NETs. The supernatant prepared at 200 ng/mL of dsDNA was used as NETs-containing medium.

To detect NETs in subcutaneous adipose tissue, the tissues embedded in optimal cutting temperature (OCT) compound (Sakura Finetek Japan, Tokyo, Japan) were frozen and sliced into 10-μm thickness sections with a cryostat (POLAR-DM, Sakura Finetek Japan). The sections were fixed with 10% Formalin Neutral Buffer Solution (FUJIFILM Wako Pure Chemical) for 10 min at room temperature, blocked non-specific antibody binding with 1% donkey serum (FUJIFILM Wako Pure Chemical) for 30 min at room temperature, and immunolabelled with primary antibodies for overnight at 4℃ followed by secondary antibodies for 1 hour at room temperature. The primary antibodies used were goat anti-myeloperoxidase (5 μg/mL, R&D systems) as a neutrophil marker, and rabbit anti-histone H3 (citrulline R2 + R8 + R17) (1 μg/mL, Abcam, Cambridge, UK) as a extracellular trap marker. The secondary antibodies used were Alexa Fluor Plus donkey anti-goat 488, and Alexa Fluor Plus donkey anti-rabbit 555 (Thermo Fisher Scientific). After the immunolabelling, the sections were mounted with ProLong gold antifade mountant with DAPI (Thermo Fisher Scientific). The images of the sections were obtained with a fluorescence microscope (BZ-X800, KEYENCE, Osaka, Japan). The imaging conditions on each channel were kept consistent. For each condition, six randomly selected images were acquired and used to count NETs.

2.7. Statistical analysis

All data are presented as the mean values with the standard error of the mean (SEM), with significance as $p < 0.05$. Statistical significance between two experimental groups was determined by paired t-test. Statistical significance among three experimental groups was determined by Tukey honestly significant difference (HSD) or Dunnett's test.

3. Results

3.1. *Ex vivo* co-cultured experimental model substitute for ASCs injection treatment

To investigate a series of biological responses that occur in ASCs-injected skin, we developed an *ex vivo* culture model using fresh excised human subcutaneous adipose tissue and ASCs (Figure 1A). To prevent ASCs-independent reactions associated with injection treatment, such as physical stimulation, we selected a co-culture experiment. We hypothesized that the efficacy of ASCs injection treatment was caused by extracellular soluble factors, because ASCs release various extracellular soluble factors, such as HGF reported previously [16]. Our experimental model was available for gene expression analysis and confocal fluorescence microscopy. ASCs co-culture was performed for a maximum of 7 days, when cells in the tissue were viable. Subcutaneous adipose tissue cultured in the absence of ASCs was designated as control.

To confirm that our experimental model was an alternative to subcutaneous adipose tissue after ASCs injection treatment, we analyzed changes in the fibrous structures from the aspect of both collagen degradation and synthesis. Staining with a fluorescent CHP probe that binds to the loosened triple strands of collagen demonstrated transient increase of collagen degradation signals after 3 days of ASCs co-culture (Figure 1B). Immunofluorescence imaging demonstrated that collagen synthesis signals increased over the course of co-culture period and were strongest after 7 days of co-culture with ASCs, at the maximum culturing period (Figure 1C). This transient collagen degradation followed by synthesis suggest a rebuilding of fibrous components in the subcutaneous adipose tissue. Thus, this model reflects the initial process of rebuilding initiated by ASCs.

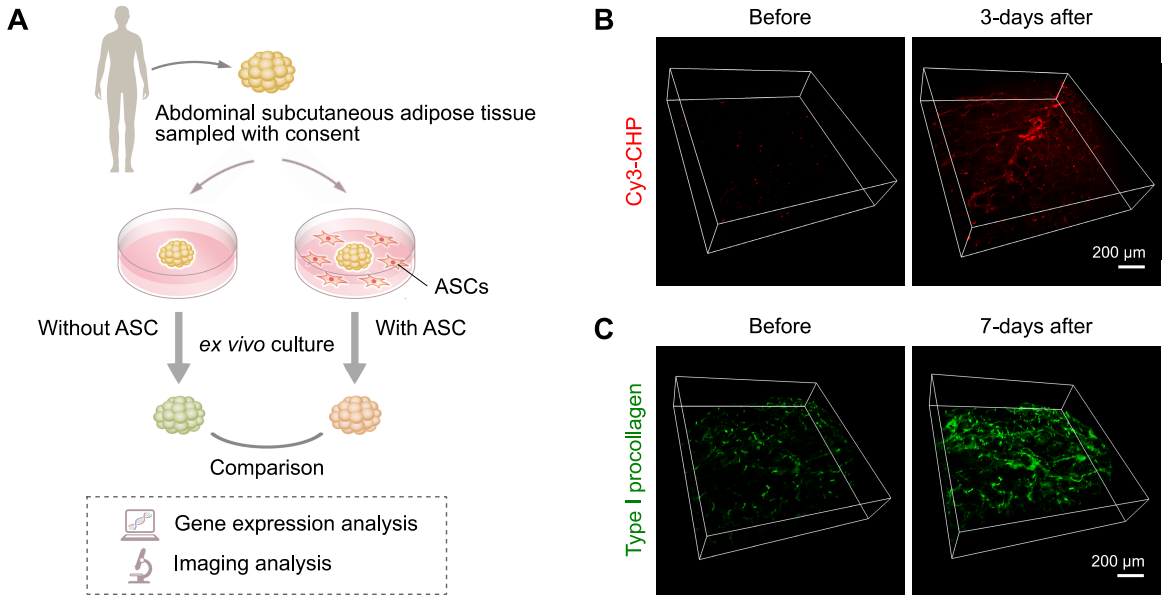

Figure 1: Establishment of an *ex vivo* experimental model.

(A) Schematic illustration of our experimental model. Fresh abdominal subcutaneous adipose tissues obtained from informed consent subjects were cultured in the presence or absence of ASCs. The cultured tissues were subjected to gene expression analysis and confocal microscopy analysis. (B-C) Observation of fibrous structural changes in *ex vivo* experimental model. Fresh subcutaneous adipose tissue was co-cultured with ASCs, and fluorescent signals of degradation (B) and synthesis (C) of type I collagen were detected in the same areas before and after culture. Degradation was observed after 3 days, and synthesis was observed after 7 days of culture. Each observation was performed for six independent visual fields, and representative images are shown here.

3.2 Wound healing processes progress in the experimental model

To overview the changes in gene expression, fresh subcutaneous adipose tissue cultured in our experimental model was collected at different time-points and had its RNA samples sequenced. For each group with and without ASCs, DEGs of Day 2, 3 and 7 were extracted by comparing their expression levels at Day 1 (Figure 2A). Our results showed changes in both groups, namely, the number of DEGs depended on culture days. This indicates that the event in our experimental model changed sequentially as culture days progressed in both the presence and absence of ASCs (Figure 2B-G). Interestingly, in both groups, GO terms related to cell proliferation (day 2 and 3) and ECM construction (day 7) were the terms that increased most (Figure 2C-E). GO terms related to inflammatory response were ranked as the top terms that decreased after 7 days of culture (Figure 2G). This means the inflammatory state peaked

out over the culture time, followed by the proliferative reaction on day 2, and thereafter the tissue moved toward ECM construction. On the other hand, a difference in the inflammation state after 7 days of culture was observed; some inflammation-related genes continued to increase in the absence of ASCs (Figure 2D), while a larger number of inflammation-related genes began to decrease in the presence of ASCs (Figure 2F). These changes in gene expression are in line with the steps of wound healing (i.e., inflammation, proliferation, and reconstruction) [17], indicating that the wound healing response progresses with the passage of days of culture in our experimental model. Thus, this model reproduced the wound healing response after damage, as it happens in the skin after aesthetic treatments.

3.3 Early termination in inflammatory gene expression by the presence of ASCs

We next analyzed the DEGs with the co-cultivation of ASCs using the gene expression without ASCs as a control, to understand the influence of the co-cultivation of ASCs on the gene expression of subcutaneous adipose tissue. The number of DEGs decreased to around 30% after the second day of culture (Figure 3A-B). After 1 day of culture, suppression of the Notch signaling pathway, a known pro-fibrotic signal, and of muscle/cytoskeleton-related functional terms including α-SMA, a myofibroblast marker, were detected, indicating that suppression of fibrotic signaling is beginning in the early stages of culture with ASCs (Figure 3C). After 3 days of culture, the functional terms related to ECM disassembly, exemplified by MMPs and other degradative enzymes, were enhanced, and the functional term related to the elastic fiber assembly was suppressed, which is consistent with the microscopic observation of a transient increase in collagen degradation after 3 days of ASCs co-culture (Figure 3E). From the second day of culture onward (Figure 3D), particularly on day 7 (Figure 3F), suppression of inflammatory responses, especially neutrophil activation, was observed. Furthermore, according to KEGG, which is a database on signal transduction systems, “suppression of pathways related to Neutrophil extracellular traps” was selected as a top pathway ($p = 4.5 \times 10^{-6}$). This suggests that ASCs contributes to the improvement of inflammatory state, acting on neutrophils.

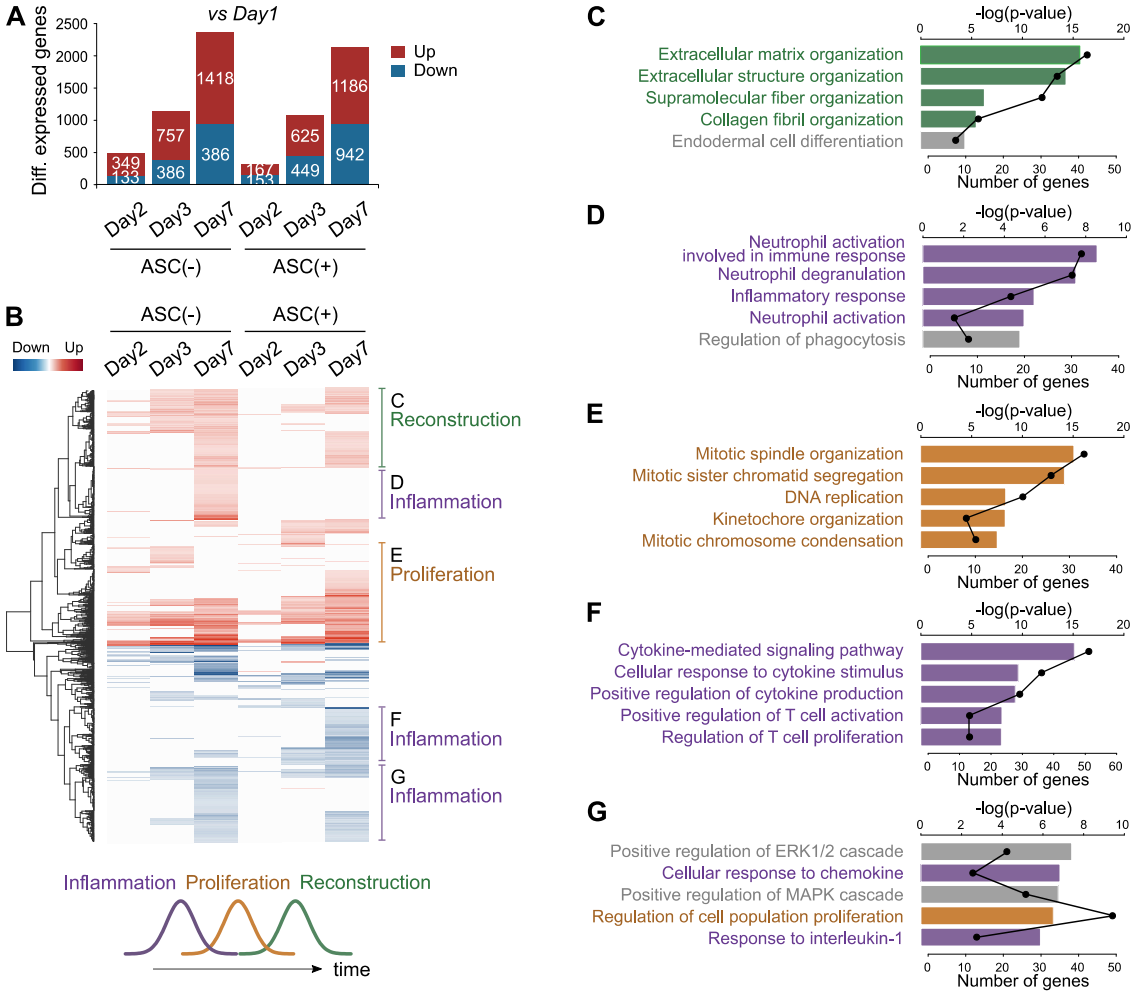

Figure 2: Analysis of time-series changes in gene expression.

Fresh subcutaneous adipose tissues from 5 donors were cultured with or without ASCs. Gene expressions after 1-, 2-, 3- and 7-days of culture were analyzed by RNA-seq. (A) Number of differentially expressed genes (DEGs, > 1.5-fold changes and < 0.05 false discovery rate) on each culture day against 1 day of culture. Red indicates up-regulated genes, blue indicates down-regulated genes. (B) A heatmap of DEGs on each culture day. Horizontal axis indicates days of culture, vertical axis indicates genes. Gene Ontology (GO) enrichment of each cluster was analyzed and the functions they represent are outlined on the right side. A schematic of the time-series changes is shown at the bottom. (C-G) The top 5 GO biological process for each cluster, shown in (B). The bar graph and upper axis represents the -log of the p-value. The line graph and lower axis represents the number of DEGs belonging to that category.

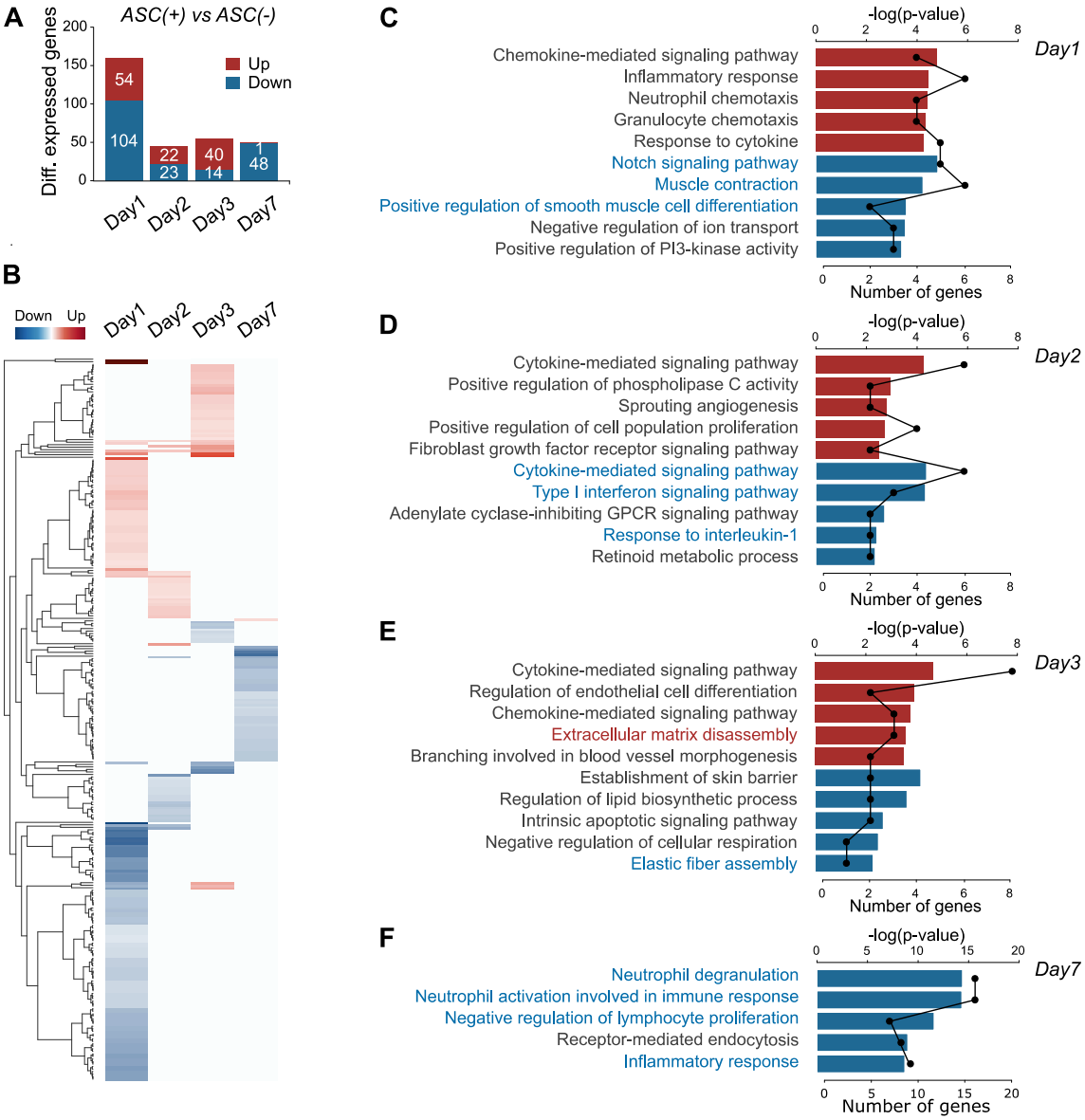

Figure 3: Analysis of changes in gene expression associated with the presence of ASCs.

The RNA-seq data same as in Figure 2 were analyzed. (A) Number of DEGs (> 1.5-fold changes and < 0.05 false discovery rate) with ASCs compared to without ASCs on each culture day. Red indicates up-regulated genes, blue indicates down-regulated genes. (B) A heat map of DEGs on each culture day. Horizontal axis indicates days of culture, vertical axis indicates genes. (C-F) Functional analysis of DEGs by GO term on each culture day. For the up- or down-regulated genes, the top 5 GO biological process were extracted and graphed. Bar graph and upper axis shows the -log of the p-value. Line graph and lower axis shows the number of DEGs belonging to that category. GO terms mentioned in the text are shown in color.

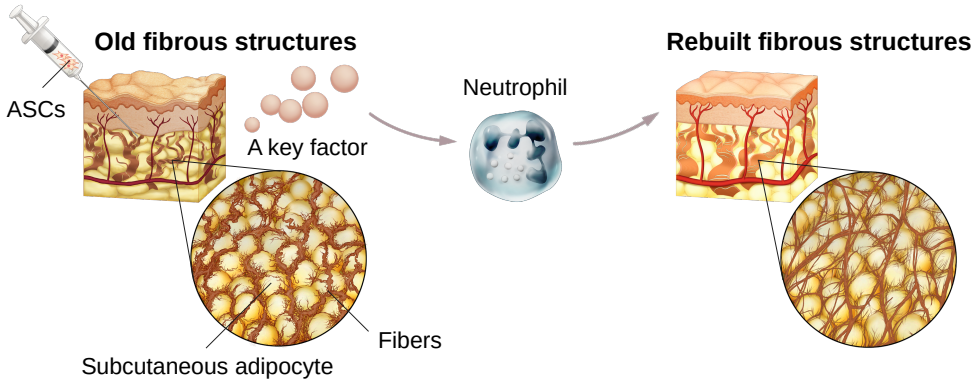

Figure 4: Schematic diagram of the validation.

There is a key factor which acts as a switch in the series of phenomena triggered by ASCs (validated in Figures 4 and 5). The key factor may act on neutrophils to regulate inflammation, thereby leading to rebuilding (validated in Figure 6).

Together, these results suggest that the wound healing process occurs sequentially in this model, and that ASCs co-culture acts to terminate the inflammatory step earlier. Thus, we hypothesize that in the absence of ASCs, the inflammatory state associated with neutrophil activation persists, which may negatively affect tissue rebuilding (Figure 4).

3.4. TSG-6 was selected as a candidate key factor for tissue rebuilding

To select candidate factors leading to tissue rebuilding, we performed in silico biological network analysis. Our results suggest that the rebuilding step is induced by a sequence of multiple phenomena. We hypothesized that regulating the factors or phenomena which change prior to these sequential events may act as a switch to trigger a series of rebuilding events. Therefore, a biological network was created for the 158 DEGs against the group without ASCs after 1 day of culture, together with proteins selected from the database that have been reported to interact directly with them in adipose tissue (Figure 5A). For each protein, the degree centrality (corresponding to the number of proteins interacting directly on the network) was calculated as a measure of its ability to act as the center of the network. We considered that the key factor should affect other cells and focused on paracrine factors among DEGs, and created a ranking of their degree centrality. Among the 24 paracrine factors, TSG-6, one of the major anti-inflammatory factors secreted by ASCs [18], showed the highest value (Figure 5B). Hence, TSG-6 may act as a hub gene in the rebuilding phenomenon.

To evaluate whether TSG-6 drives genes involved in fibrous structural remodeling, we examined the function of genes whose expression varied along with TSG-6 in subcutaneous adipose tissue. RNA-seq was performed on cheek subcutaneous adipose tissues collected from 9 donors, and genes highly correlated with TSG-6 expression were extracted (Pearson's correlation coefficient, $r > 0.7$). The functions of the 245 extracted genes were ranked by GO terms (Figure 5C). Immune responses, which are known to be regulated by TSG-6, were selected as the top functions, confirming the validity of this correlation analysis. Simultaneously, several terms related to ECM organization were selected, and some genes classified in these terms were involved in the synthesis and degradation of fibrous structures. This result suggests that subcutaneous adipose tissue with high TSG-6 expression promotes fibrous structures degradation and synthesis (i.e., rebuilding). TSG-6 may be closely involved in building fibrous structures in subcutaneous adipose tissue.

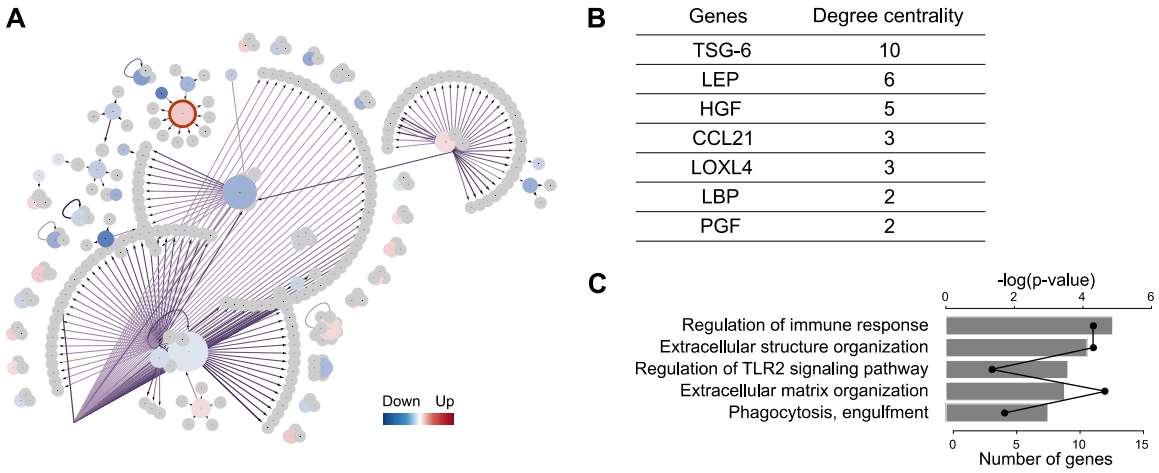

Figure 5: Using biological network analysis to identify a key factor involved in rebuilding.

(A) The protein-protein interaction (PPI) network of DEGs on 1 day of ASCs co-culture. Nodes indicate proteins. Edges indicate direct PPI. Node size depends on the number of edges. Red and blue nodes indicate proteins with significantly increased and decreased expression, respectively, while gray nodes indicate proteins extracted from the database that bind directly to DEGs in adipose tissue. The color intensity of the edges indicates the reliability of the PPI. TSG-6 is highlighted with framing. (B) Ranking of paracrine factors with high degree centrality among DEGs after 1 day of culture. (C) Functional analysis of TSG-6 co-expressed genes by GO term. RNA-seq was performed on cheek subcutaneous adipose tissue (N=9). TSG-6 co-expressed genes were extracted according to the criteria of Pearson's correlation coefficient greater than 7.0. The top 5 GO biological process were extracted and graphed. The bar graph and upper axis represents the -log of the p-value. The line graph and lower axis represents the number of genes belonging to that category.

3.5. TSG-6 inhibits fibrosis and promotes proper remodeling of fibrous structures

To demonstrate that TSG-6 is the key factor of rebuilding, the rebuilding response following suppression of TSG-6 function was examined. Functional suppression of TSG-6 was performed by co-culturing fresh subcutaneous adipose tissue with ASCs by adding TSG-6 neutralizing antibody to the medium. First, fibrous structural changes were observed by confocal microscopy over time. The fluorescent images of the same area taken before and after culture were quantified with the signal intensity and graphed (Figure 6A-B). Degradation of type I collagen, as detected by CHP signals, was increased more than 1.5-fold after 3 days of ASCs co-culture, while no significant change was observed in the absence of ASCs. This effect of ASCs on degradation was significantly suppressed by the addition of TSG-6 neutralizing antibody (Figure 6A). Synthesis of type I collagen detected by antibody staining of type I procollagen increased after 7 days of culture, regardless of the presence or absence of ASCs, but the level of increase was significantly higher in the absence of ASCs. This effect of ASCs on synthesis was also significantly inhibited by the addition of TSG-6 neutralizing antibody (Figure 6B), suggesting that the effect of ASCs co-culture on inducing type I collagen degradation and synthesis is both mediated by TSG-6. In addition, high collagen synthesis observed in the absence of ASCs was hypothesized to be related to fibrosis.

Next, to investigate the relationship between collagen synthesis and fibrosis in our experimental model, the expression changes of fibrosis-related genes in our experimental model were verified. Fresh subcutaneous adipose tissue was cultured under the following three conditions: without ASCs, with ASCs, and with ASCs and TSG-6 neutralizing antibody, and qPCR was performed on the collected tissue. The expression of α-SMA, a marker of myofibroblasts that acts as a key player in fibrosis, was significantly decreased upon ASCs co-culture, and this effect of ASCs was significantly suppressed by the addition of TSG-6 neutralizing antibody (Figure 6C). In the absence of ASCs, collagen synthesis accompanied by α-SMA induction was observed, suggesting that the tissue may move toward fibrosis in the future. On the other hand, in the presence of ASCs, collagen synthesis without α-SMA induction was promoted after transient degradation due to TSG-6-mediated effects, suggesting that the rebuilding phenomenon was initiated.

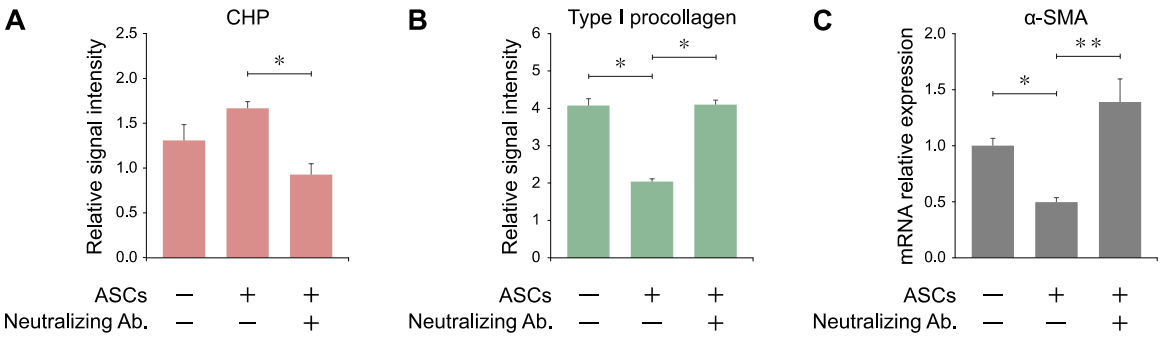

Figure 6: TSG-6 is as key factor in tissue rebuilding.

(A-B) The observation of fibrous structural changes in *ex vivo* experimental model when adding TSG-6 neutralizing antibody. Fresh subcutaneous adipose tissue was cultured: without ASCs, with ASCs, and with ASCs and TSG-6 neutralizing antibody. Fluorescent signals of degradation (A) and synthesis (B) of type I collagen were detected before and after culture. Degradation and synthesis were observed after 3 and 7 days, respectively. Observations were performed for four or five independent visual fields, and signal intensities were quantified. (C) Quantitative PCR (qPCR) for a fibrosis-promoting factor. Fresh subcutaneous adipose tissues were cultured: without ASCs, with ASCs, and with ASCs and TSG-6 neutralizing antibody (N=4). Tissues were collected after 1 day of culture and subjected to qPCR. Mean + SE, Tukey HSD test, *p < 0.05, **p<0.01

3.6. TSG-6 inhibits fibrosis by suppressing NETs formation

Finally, we examined how TSG-6 regulates rebuilding. Based on the result of gene expression analysis showing suppression of neutrophil activation by ASCs, we focused on neutrophil, especially NETs. We hypothesized that TSG-6 regulates rebuilding through NETs.

To understand the effect of TSG-6 on NETs formation, we examined the correlation between TSG-6 expression and the number of NETs in subcutaneous adipose tissue. Each cheek subcutaneous adipose tissue collected from 15 donors was divided into two pieces, for which TSG-6 expression verification and immunohistochemical staining detection and counting of NETs. TSG-6 expression and the number of NETs per region of interest showed weak negative correlations, indicating that the higher the expression of TSG-6 in subcutaneous adipose tissue, the fewer the number of NETs (Figure 7A). To verify the possibility that TSG-6 inhibits NETs formation, we tested it in a more direct system. Isolated human neutrophils were induced to form NETs, and the addition of TSG-6 recombinant protein inhibited NETs formation in a concentration-dependent manner (Figure 7B), indicating that TSG-6 inhibits NETs formation. To verify whether TSG-6 suppresses NETs

formation in our experimental model, NETs in fresh subcutaneous adipose tissue co-cultured with ASCs were analyzed immunohistologically. Graphical depiction of the number of NETs per unit area revealed that the number of NETs was significantly reduced in the presence of ASCs, indicating that ASCs inhibit NETs formation (Figure 7C). In subcutaneous adipose tissues co-cultured with ASCs in the presence of TSG-6 neutralizing antibody, the number of NETs was recovered at the same level as in the absence of ASCs, suggesting that ASCs inhibit the formation of NETs via TSG-6 in subcutaneous adipose tissue.

To investigate the effects of exposure to NETs on the fibrous structures of subcutaneous adipose tissue, gene expression changes in subcutaneous adipose tissue exposed to NETs were examined. In brief, neutrophils were stimulated to induce NETs, and the released NETs were collected as culture supernatant. Subcutaneous adipose tissue was cultured with NETs-containing medium for 48 hours and subjected to qPCR. Exposure to NETs significantly increased the expression of type I collagen and α-SMA in subcutaneous adipose tissue (Figure 7D). This suggests that subcutaneous adipose tissue exposed to NETs is promoted to change in the direction of fibrosis, resulting in inhibition of remodeling. Together, in subcutaneous adipose tissue, ASCs inhibit NETs formation via TSG-6. This effect was considered to inhibit subcutaneous adipose tissue to progress toward fibrosis and to determine the direction towards tissue rebuilding.

4. Discussion

Subcutaneous injection of ASCs rebuilds skin fibrous structures, exerting superior effects than current cosmetics on aging skin problems. Here, we elucidated the mechanism of skin improvement by ASCs injection, thereby going beyond the realm of cosmetics that had been developed through mechanistic research biased towards investigating the causes of skin problems, whose main appeal is “deterioration suppression”. We identified TSG-6, a key factor in triggering tissue rebuilding, by elucidating a series of biological responses occurring in subcutaneous adipose tissues co-cultured with ASCs. When tissue damage occurs in subcutaneous adipose tissues, neutrophils form NETs, resulted in a persistent inflammatory state and accelerated fibrosis. On the other hand, ASCs inhibits NET formation via TSG-6. This promotes transient collagen degradation as well as collagen synthesis not directed toward fibrosis, which may determine the shift toward rebuilding (Figure 8).

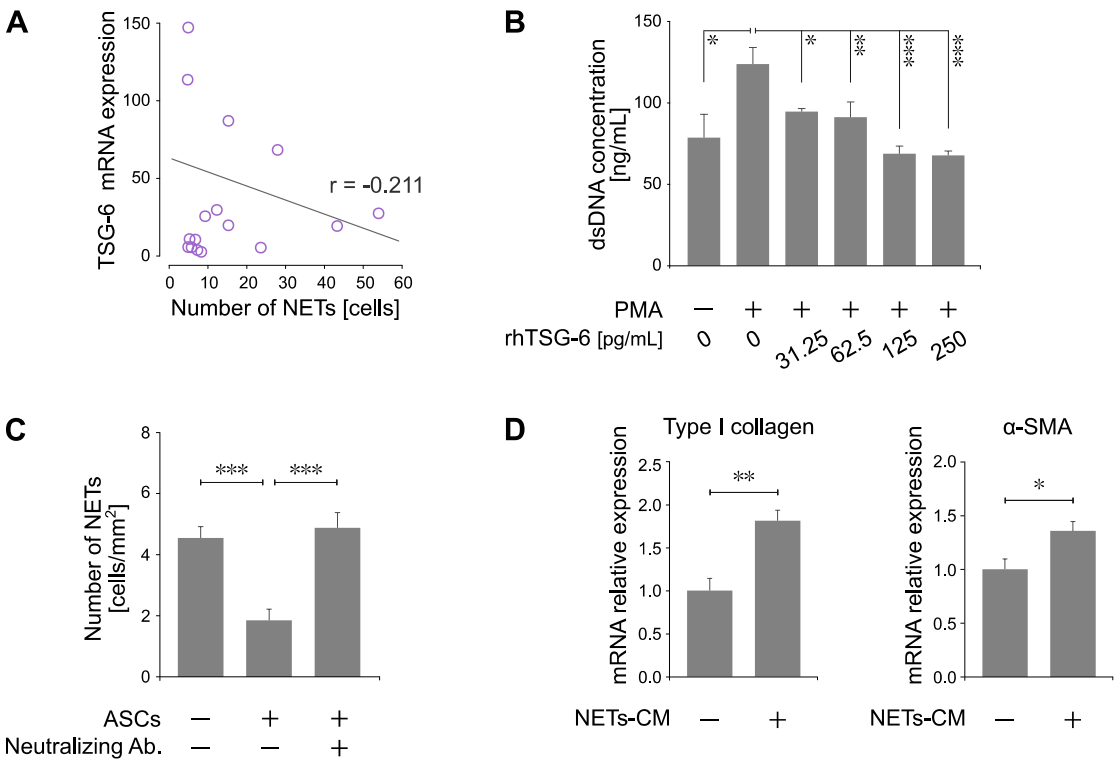

Figure 7: Analyses of the effect of NETs on fibrous structures of subcutaneous adipose tissue.

(A) Correlation analysis of TSG-6 expression and the number of NETs in subcutaneous adipose tissue. Each cheek subcutaneous adipose tissue collected from 15 donors was divided into two pieces. One was subjected to qPCR to quantify TSG-6 expression, and the other was immunohistochemically stained to detect and count NETs. TSG-6 mRNA expression and the number of NETs were plotted, and Pearson correlation coefficient (r) was calculated. (B) Analysis of the effect of TSG-6 on NETs formation. NETs were induced by adding 50 nM Phorbol 12-myristate 13-acetate to cultured neutrophils which preliminary incubated with 31.25-250 pg/mL TSG-6 recombinant protein for 15 minutes. After 1 hour of culture, the amount of NETs formed was measured using dsDNA as an indicator. N=4, Mean + SE, Dunnett's test, *p < 0.05, **p < 0.01, ***p < 0.001. (C) Numbers of NETs in immunohistochemical staining images. Fresh subcutaneous adipose tissues were cultured under the following three conditions: without ASCs, with ASCs, and with ASCs and TSG-6 neutralizing antibody. Tissues were immunohistochemically stained after 1 day of culture. The number of NETs was counted from six independent specimens in each group. Mean + SE, Tukey HSD test, ***p < 0.001. (D) Effect of NETs on fibrosis-related gene expression in subcutaneous adipose tissue. NETs were induced in neutrophils and the culture supernatant containing NETs was collected. Expression of fibrosis-related genes in fresh subcutaneous adipose tissue cultured with the supernatant containing NETs was quantified by qPCR. CM; conditioned medium. N=4, Mean + SE, paired t-test, *p < 0.05, **p < 0.01.

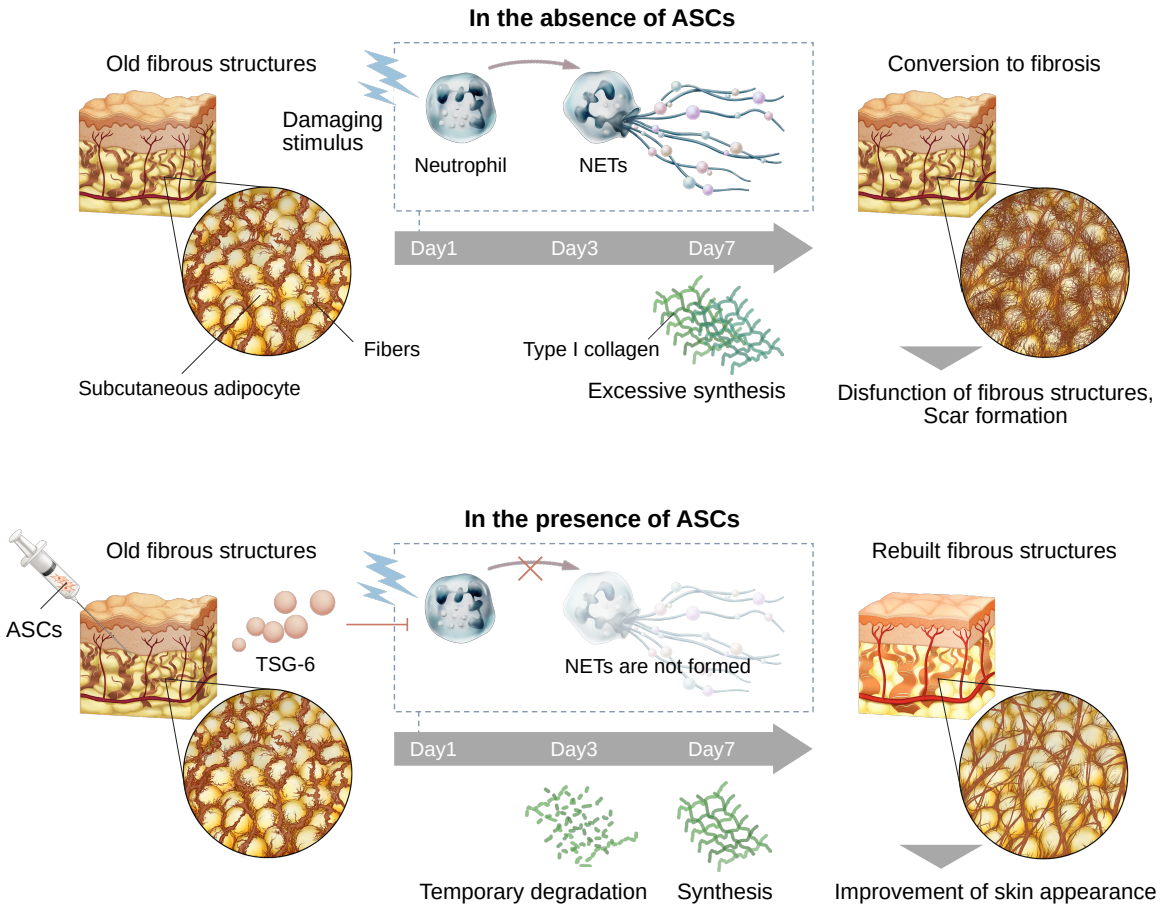

Figure 8: Conceptual diagram of this study.

In the absence of ASCs, neutrophils form NETs in damaged subcutaneous adipose tissue; NETs cause excessive synthesis of type I collagen and mediate the transition to fibrosis. In the presence of ASCs, TSG-6 released from ASCs inhibits the formation of NETs. This induces transient degradation and subsequent synthesis of type I collagen resulting in tissue rebuilding.

Our experimental model demonstrated sequential wound healing process depending on culture days. Previous studies have reported that ASCs-injected skin leads to tissue damage, bleeding, inflammation, and ischemic conditions [19], [20]. Since the tissue used in our model was collected from living bodies, tissue damage has occurred. Subsequent culture starting several hours after sampling provides an environment allowing biological responses to continue; therefore, the wound healing process was similar to skin that underwent treatment. Whereas, one limitation of our model is the absence of blood circulation, since the excised tissue is cultured. This study suggests that NETs mediated response, but the response

in vivo may be amplified beyond that observed in our model because there is additional neutrophil recruitment.

Analysis of gene expression changes revealed that the co-culture with ASCs may end the inflammatory response earlier, suggesting ASCs may affect the inflammatory phase of the wound healing process. When proper progression of the wound healing process is prevented, it is reported to be impaired and to occur excessive deposition of ECM. One reason is prolonged inflammatory phase prevents the shift to the proliferative and even reconstructive phases, thereby disrupting the balance of the ECM construction [21]. ASCs are known to have immunomodulatory capacity and to influence various cell types involved in inflammation [22], [23], [24]. ASCs may play a role in suppressing an excessive and prolonged inflammatory phase in the wound healing process through their immunomodulatory capacity, thereby promoting the shift to the proliferative and reconstructive phases, which in turn may lead to rebuilding.

TSG-6, first identified as a key factor for rebuilding in this study, is one of the major anti-inflammatory factors secreted by ASCs. A previous report using skin wounding model mice suggested TSG-6 is related to wounding closure and suppresses fibrosis [25], which is consistent with the findings observed in this study.

As a mechanism of inflammatory regulation by TSG-6, effects on multiple immune system cells have been reported [26], [27], [28]. In the relationship between TSG-6 and neutrophils, which was focused on this study, TSG-6 produced by human amnion-derived mesenchymal stem cells has been reported to inhibit the formation of NETs [29]. NETs are structures formed by neutrophils releasing intracellular substances such as chromatin skeletons and granulocyte proteins into the extracellular space [30]. While this is one of the biological defense systems, excessive NETs have been reported to be associated with chronic inflammation and fibrosis in some organs [31]. This is the first report to demonstrate that TSG-6 suppresses NETs in subcutaneous adipose tissue, thereby inhibiting the transition to fibrosis and inducing a switch to rebuilding.

This study was conducted on subcutaneous adipose tissue, but fibrous structures also exist in the dermis, and we believe that our findings are applicable to the dermis as well. We expect that expanding our research will further expand our understanding of the rebuilding phenomenon.

In summary, our findings are useful for promoting the development of cosmetics with superior effects for various skin issues caused by changes of fibrous structures such as wrinkling and sagging. Furthermore, it has the potential of expanding applications of cosmetics on fibrotic skin problems such as an acne scars, that are believed to be challenging to treat. In addition to cosmetics, TSG-6 control is also expected to be applied to aftercare to reduce downtime and to maximize efficacy in aesthetic medicine and to scar reduction in the medical field.

5. Conclusion

From our result, TSG-6 is a key factor that improves the inflammatory state of tissues by inhibiting the formation of NETs in subcutaneous adipose tissue. In turn, it drives tissue state from the direction of fibrosis towards rebuilding. In addition, this study pioneers a new approach elucidating the biological mechanisms underlying skin improvement to make it possible to “restore the skin to its younger state”, instead of the solutions to “stop the aging process”. In all, this study paves the way for developing innovative cosmetics that go far beyond conventional cosmetics.

6. Acknowledgments

We would like to show our greatest appreciation to the members of the Frontier Research Center of POLA Chemical Industries for their fruitful discussions and advising in the experiments.

7. Conflict of Interest Statement

This study was funded by POLA Chemical Industries.

8. References

1. Mora Huertas AC et al (2016) Molecular-level insights into aging processes of skin elastin. Biochimie. 128–129:163–173.
2. J Varani et al (2001) Inhibition of type I procollagen synthesis by damaged collagen in photoaged skin and by collagenase-degraded collagen in vitro. Am J Pathol. 158(3) 931–942.

3. J Varani et al (2006) Decreased collagen production in chronologically aged skin: roles of age-dependent alteration in fibroblast function and defective mechanical stimulation. Am J Pathol. 168(6) 1861–1868.
4. Charles-de-Sa L et al (2015) Antiaging treatment of the facial skin by fat graft and adipose-derived stem cells. Plast Reconstr Surg. 135: 999–1009.
5. Yoshimura K (2010) Regenerative medicine with adipose stem/progenitor cells: Application to cosmetic dermatology. Aesthetic Dermatol. 20: 225–236.
6. Luiz Charles-de-Sá et al (2015) Antiaging Treatment of the Facial Skin by Fat Graft and Adipose-Derived Stem Cells. Plast Reconstr Surg. 135(4) 999–1009.
7. Luan A et al (2016) Cell-Assisted Lipotransfer Improves Volume Retention in Irradiated Recipient Sites and Rescues Radiation-Induced Skin Changes. Stem Cells. 34(3) 668–673.
8. Andrews S (2010) FastQC: a quality control tool for high throughput sequence data.
9. Kim D et al (2015) HISAT: a fast spliced aligner with low memory requirements.
10. Mortazavi A et al (2008) Mapping and quantifying mammalian transcriptomes by RNA-Seq. Nature methods. 5(7) 621–628.
11. Love M et al (2015) Differential analysis of count data-the DESeq2 package.
12. Chen EY et al (2013) Enrichr: interactive and collaborative HTML5 gene list enrichment analysis tool. BMC Bioinformatics. 128(14)
13. Kuleshov MV et al (2016) Enrichr: a comprehensive gene set enrichment analysis web server 2016 update. Nucleic Acids Res. 44(W1) W90–W97.
14. G Alanis-Lobato et al (2017) HIPPIE v2.0: enhancing meaningfulness and reliability of protein-protein interaction networks. Nucleic Acids Res. 45(D1) D408–D414.
15. Shannon P et al (2003) Cytoscape: a software environment for integrated models of biomolecular interaction networks. Genome Research. 13(11) 2498–2504.
16. Kim WS et al (2009) Protective role of adipose-derived stem cells and their soluble factors in photoaging. Arch Dermatol Res. 301(5) 329–336.
17. P Martin (1997) Wound healing -aiming for perfect skin regeneration. Science. 276(5309) 75–81.
18. Lee RH et al (2014) TSG-6 as a biomarker to predict efficacy of human mesenchymal stem/progenitor cells (hMSCs) in modulating sterile inflammation in

vivo. Proceedings of the National Academy of Sciences. 111(47) 16766–16771.

19. Yoshimura K et al (2009) Adipose-derived stem/progenitor cells: roles in adipose tissue remodeling and potential use for soft tissue augmentation. Regen Med. 4: 265–273.
20. Suga H et al (2009) IFATS collections: FGF-2-induced HGF secretion by adipose-derived stromal cells inhibits post-injury fibrogenesis through a JNK-dependent mechanism. Stem Cells. 27: 238–249.
21. Loots MAM et al (1998) Differences in Cellular Infiltrate and Extracellular Matrix of Chronic Diabetic and Venous Ulcers Versus Acute Wounds. J Investig Dermatol. 111: 850–857.
22. Baharlou R et al (2017) Human adipose tissue-derived mesenchymal stem cells in rheumatoid arthritis: Regulatory effects on peripheral blood mononuclear cells activation. Int. Immunopharmacol. 47: 59–69.
23. Anderson P et al (2017) Allogeneic Adipose-Derived Mesenchymal Stromal Cells Ameliorate Experimental Autoimmune Encephalomyelitis by Regulating Self-Reactive T Cell Responses and Dendritic Cell Function. Stem Cells Int. 1–15.
24. Franquesa M et al (2015) Human Adipose Tissue-Derived Mesenchymal Stem Cells Abrogate Plasmablast Formation and Induce Regulatory B Cells Independently of T Helper Cells. Stem Cells. 33: 880–891.
25. Yu Qi et al (2014) TSG-6 released from intradermally injected mesenchymal stem cells accelerates wound healing and reduces tissue fibrosis in murine full-thickness skin wounds. J Invest Dermatol 134(2) 526–537.
26. Song W-J et al (2017) TSG-6 secreted by human adipose tissue-derived mesenchymal stem cells ameliorates DSS-induced colitis by inducing M2 macrophage polarization in mice. Scientific Reports. 7(1) 5187.
27. Mittal M et al (2016) TNFα-stimulated gene-6 (TSG6) activates macrophage phenotype transition to prevent inflammatory lung injury. Proceedings of the National Academy of Sciences. 113(50) E8151–E8158.
28. Douglas P Dyer et al (2014) TSG-6 inhibits neutrophil migration via direct interaction with the chemokine CXCL8. J Immunol. 192(5) 2177–2185.
29. Fátima Sofia Magana-Guerrero et al (2017) Human Amniotic Membrane

Mesenchymal Stem Cells inhibit Neutrophil Extracellular Traps through TSG-6. Sci Rep. 7: 12426.

30. Brinkmann V et al (2004) Neutrophil extracellular traps kill bacteria. Science. 303(5663) 1532–1535.

31. A Chrysanthopoulou et al (2014) Neutrophil extracellular traps promote differentiation and function of fibroblasts. J Pathol. 233(3) 294–307.